

**Surface Plasmon Resonance Spectroscopy-Based Process Sensors**  
**S. McWhorter, Brian B. Anderson and K. Zeigler**

Unclassified  
Does Not Contain Unclassified Controlled Nuclear Information (UCNI)

July 30, 2003

**Westinghouse Savannah River Company**  
**Savannah River Site**  
**Aiken, SC 29808**

---



WSRC-TR-2003-00290  
Revision 0

Keywords:  
Moisture, Hydrogen, Thin Film, SPR

Classification: U

## **Surface Plasmon Resonance Spectroscopy-Based Process Sensors**

**Westinghouse Savannah River Company  
Savannah River Site  
Aiken, SC 29808**

---



**This document was prepared in conjunction with work accomplished under Contract No. DE-AC09-96SR18500 with the U. S. Department of Energy.**

#### **DISCLAIMER**

**This report was prepared as an account of work sponsored by an agency of the United States Government. Neither the United States Government nor any agency thereof, nor any of their employees, makes any warranty, express or implied, or assumes any legal liability or responsibility for the accuracy, completeness, or usefulness of any information, apparatus, product or process disclosed, or represents that its use would not infringe privately owned rights. Reference herein to any specific commercial product, process or service by trade name, trademark, manufacturer, or otherwise does not necessarily constitute or imply its endorsement, recommendation, or favoring by the United States Government or any agency thereof. The views and opinions of authors expressed herein do not necessarily state or reflect those of the United States Government or any agency thereof.**

**This report has been reproduced directly from the best available copy.**

**Available for sale to the public, in paper, from: U.S. Department of Commerce, National Technical Information Service, 5285 Port Royal Road, Springfield, VA 22161,  
phone: (800) 553-6847,  
fax: (703) 605-6900  
email: [orders@ntis.fedworld.gov](mailto:orders@ntis.fedworld.gov)  
online ordering: <http://www.ntis.gov/help/index.asp>**

**Available electronically at <http://www.osti.gov/bridge>  
Available for a processing fee to U.S. Department of Energy and its contractors, in paper, from: U.S. Department of Energy, Office of Scientific and Technical Information, P.O. Box 62, Oak Ridge, TN 37831-0062,  
phone: (865)576-8401,  
fax: (865)576-5728  
email: [reports@adonis.osti.gov](mailto:reports@adonis.osti.gov)**

**ABSTRACT**

The Analytical Development Section (ADS) of the Savannah River Technology Center (SRTC) developed a novel, monolithic surface plasmon resonance (SPR) probe for process monitoring as part of the Defense Programs Plant Directed Research and Development Program. The sensor incorporates multi-layer thin films on a fused-silica hemispherical lens. The simple optical design of the device increases robustness and fabrication precision and allows for sensitive SPR measurements to be made without complex polarizing and collimating optics. The utility of the probe is demonstrated for sensing moisture and hydrogen in process environments. This device is capable of optically detecting moisture from <1% (750ppb) to 100% and hydrogen concentrations from at least 0.1% to the explosive limit (4%) with a calculated limit of detection for H<sub>2</sub> of 0.102% (signal-to-noise (S/N) = 3 criteria). Theoretical optical modeling of the SPR system and room temperature performance characteristics of the sensor are reported.

## **TABLE OF CONTENTS**

<b>ABSTRACT .....</b>	<b>4</b>
<b>1.0 SUMMARY.....</b>	<b>7</b>
<b>2.0 INTRODUCTION .....</b>	<b>7</b>
2.1 BACKGROUND .....	7
2.2 SURFACE PLASMON RESONANCE SPECTROSCOPY .....	8
<b>3.0 EXPERIMENTAL.....</b>	<b>9</b>
3.1 CONDUCT OF TESTING .....	9
3.2 MATERIALS .....	9
3.3 SPR SENSOR APPARATUS AND CHARACTERIZATION .....	9
3.3.1 <i>Thin-film Deposition</i> .....	10
3.3.2 <i>Humidity Sensor Measurement System</i> .....	10
3.3.3 <i>Hydrogen Sensor Measurement System</i> .....	10
3.4 OPTICAL SYSTEM.....	10
<b>4.0 RESULTS AND DISCUSSION.....</b>	<b>11</b>
4.1 SPR PROBE CHARACTERIZATION.....	11
4.2 EVALUATION OF SENSOR COATINGS.....	13
4.2.1 <i>Silicon Dioxide Coatings</i> .....	13
4.2.2 <i>Palladium Hydride Coatings</i> .....	13
<b>5.0 CONCLUSIONS.....</b>	<b>15</b>
<b>6.0 ACKNOWLEDGEMENTS .....</b>	<b>15</b>
<b>7.0 REFERENCES .....</b>	<b>16</b>

## **LIST OF FIGURES**

Figure 1. Optical ray-trace of the 60° and 45° SPR probes.....	17
Figure 2. Experimental set-up for the measurement of dew point and humidity.....	19
Figure 3. Experimental apparatus for the detection of hydrogen.....	20
Figure 4. Comparison between experimental and theoretical SPR spectra.....	21
Figure 5. SPR sensor refractive index calibration.....	22
Figure 6. Short term (A-B) and long term (C-D) comparisons of the resonance wavelength obtained from the gold/silica sensor with the baseline humidity values from a capacitive RH sensor.....	23
Figure 7. Prediction results for 49 day trial, temperature corrected SPR moisture sensor.....	24
Figure 8. “Pressure-composition” isotherms for palladium versus the absorption of molecular hydrogen for various temperatures in degrees Celsius.....	25
Figure 9. Typical response for successive cycles from pure nitrogen to a 4% hydrogen concentration.....	26

## **LIST OF TABLES**

Table 1. Standard salt solutions used in Characterization of the SPR sensor to refractive index perturbations.....	18
--	----

**Surface Plasmon Resonance Spectroscopy-Based Process Sensors****by S. McWhorter, Brian B. Anderson and K. Zeigler****Westinghouse Savannah River Company****Savannah River Site****Aiken SC 29808****1.0 SUMMARY**

The Analytical Development Section (ADS) of the Savannah River Technology Center (SRTC) developed a novel, monolithic surface plasmon resonance (SPR) probe for process monitoring as part of the Defense Programs Plant Directed Research and Development Program (DP PDRD). The sensor incorporates multi-layer thin films on a fused-silica hemispherical lens. The simple optical design of the device increases robustness and fabrication precision and allows for sensitive SPR measurements to be made without complex polarizing and collimating optics. The utility of the probe is demonstrated for sensing moisture and hydrogen in process environments. This device is capable of optically detecting moisture from <1% (750ppb) to 100% and hydrogen concentrations from at least 0.1% to the explosive limit (4%) with a calculated limit of detection for H<sub>2</sub> of 0.102% (S/N=3 criteria). Theoretical optical modeling of the SPR system and room temperature performance characteristics of the sensor are reported.

**2.0 INTRODUCTION****2.1 Background**

Optical sensors have long been a goal of DOE research efforts to improve safety issues associated with weapons processes as well as to improve the control of operations where hydrogen is generated, separated and stored. Evolution of hydrogen creates flammability issues for tritium process facilities and, as such, must be closely monitored to confirm safe concentrations during operation. Of particular concern is the ability to monitor with a non-electrical, non-conducting device, concentrations approaching the lower explosive limit for hydrogen as well as measuring moisture in the same process environment.

Currently, mass spectrometry<sup>1</sup> is the preferred method for measurement of hydrogen in the Tritium Facilities at the Savannah River Site (SRS) but is impractical for multi-point measurements due to size and cost constraints. In addition, current commercially available electronic humidity sensors rely on changes in the electrical properties of a polymeric membrane, which not only poses a significant safety concern, but is also subject to interference from hydrogen. These shortcomings demonstrate the need for further advancements in the area of hydrogen and moisture process monitoring. This paper reports progress on the development of inexpensive, fiber-optic moisture and hydrogen sensors intended to meet the safety monitoring needs of the SRS Tritium Facilities.

## 2.2 Surface Plasmon Resonance Spectroscopy

Surface plasmon resonance (SPR) measurements are made using optical systems that control parameters to which SPR is sensitive, namely incident angle, wavelength of incident light, degree of polarization, and optical materials. The SPR technique is used in development and characterization of ultra-thin films<sup>2,3</sup>. In general, a typical SPR experiment requires a dielectric substrate, a prism in most cases, which has been coated with a suitable noble metal at a precise thickness. The combination of the substrate, noble metal, and sample in contact with the metal, allows for the generation and support of surface plasmon polaritons (SPPs) that are formed along the metal-dielectric interface. These polaritons are highly damped charge density waves oscillating at optical frequencies, and may be excited if the materials and optical properties of an experimental system are chosen correctly.

In general, the SPPs are not measured directly, but their presence is inferred by monitoring the light intensity reflected from the substrate/metal interface. The reflected light will contain a deep minimum in intensity, and this minimum occurs at what is termed the resonance for the surface polariton, or plasmon. The monitoring of the surface plasmon reflectivity curve, and in particular, the position of the resonance, yields what is generally known as surface plasmon resonance spectroscopy (SPRS). The position of the reflectivity minimum is very sensitive to the interface properties between the substrate face and the liquid. Changes in metal film thickness, surface adsorbed species, and liquid dielectric properties are all seen as changes in the SPR resonance wavelength. SPR has been shown to be sensitive to very low levels of material adsorbed onto a surface (much less than a monolayer).

SPRS is used to determine the optical properties of the materials which make up the structure that supports SPR, which includes the metal layer and anything in contact with the metal layer. The plasmon wave decays exponentially from the surface of the metal and penetrates into the sample approximately 200-300 nm, depending upon the materials. Different configurations have been employed with the goal of miniaturization and significant effort has been made towards the development of compact SPR systems and probe geometries that enable the collection of research or bench top quality SPR spectra from fiber optic-based sensors. Several fiber optic-based sensors have been developed for liquid phase bio-assay, most notably the multi-mode fiber based SPR probe marketed by Pharmacia<sup>4, 5</sup>. A single-mode optical fiber SPR sensor system was described by Slavík, et al. for application in liquid systems<sup>6</sup>. Also fiber coupled compact planar surface plasmon resonance transducer, which makes use of a faceted probe end, and miniature-coupling optics was described and applied to bio-sensing for evaluation<sup>7</sup>.

SRTC has developed a novel SPR fiber optic-based probe which enables the acquisition of high quality, high resolution SPR spectra using a simple and robust probe with a single bulk optical element with no facets. The SPR probe is based on a commercially available



hemispherical attenuated total reflection (ATR) spectroscopy probe (Equitech, International). The probe consists of a stainless steel 0.5-inch diameter housing, which contains optical fibers that are polished and spaced appropriately at the distal end. The fibers are arranged such that the launch and collection fibers are placed at the focal points for propagation through the ATR hemisphere. The ATR probe design takes advantage of the geometrical optics associated with internal reflections along the hemisphere, where the rays are traced along inscribed polygons (4, 5, 6 sided, etc.), to perform ATR measurements without relying on a faceted crystal. Figure 1 shows the configuration used in these SPR experiments, where the light is incident upon the hemisphere in an ATR configuration. This SPR probe allows SPR excitation at any or all of the internal reflection points along the surface without the need for external focusing or collimating optics. The monolithic construction (single optical element) and incident angle purity achieved by the hemisphere curvature yields a fiber optic coupled probe which generates research quality SPR spectra. Previously reported SPR probe configurations require additional optical components and facets to generate high quality SPR spectra.

### **3.0 EXPERIMENTAL**

#### **3.1 Conduct of Testing**

This work was part of the DP PDRD. The work was scoping in nature and involved exploratory research of new technologies. The work followed the SRTC research guidelines for exploratory activities and used a technical notebook as the primary means of documentation.

#### **3.2 Materials**

Stainless steel ATR probes and sapphire hemispheres were purchased from Equitech International and fused-silica hemispheres were purchased from A.W.I. Industries (USA) Inc. Chromium, gold and palladium sputtering targets (Kurt J Lesker Co., 99.9+% purity) were used in the fabrication for the SPR sensor elements. One-inch diameter doubly polished silicon wafers (Silicon Quest International) were used for quartz crystal microbalance (QCM) calibration and ellipsometry studies. Deionized water (Barnstead, 17.6 MOhm-cm), solid sodium chloride, sodium hydroxide pellets, methanol, and concentrated nitric acid (all Fisher, ACS reagent grade) were used to clean substrates and prepare solutions for SPR sensor characterization.

#### **3.3 SPR Sensor Apparatus and Characterization**

The SPR sensor was characterized with respect to refractive index via a series of sodium chloride solutions prepared gravimetrically in deionized water. Table 1 lists the solutions and associated calculated refractive index values at 20°C and 30°C<sup>8</sup>. The values at 30°C were calculated using the dispersion of pure water.

### **3.3.1 Thin-film Deposition**

Hemispheres of the appropriate material (i.e. fused-silica or sapphire) were cleaned and dried in a dry argon (Ar) jet and placed into sputtering masks which were made in-house. The masks allowed material to be sputtered onto specific locations of the curved hemispheres. The masks were placed into a vacuum coating system which utilizes two planar magnetron sputter sources with either direct current (DC) or radio frequency (RF) excitation of an Ar plasma. A thin (15 Å) layer of chromium was applied as an adhesion layer, followed by a layer of gold having a final thickness of 500 angstroms. In the case of humidity sensing, a silica layer was applied next using the RF source to a thickness of approximately 800 angstroms. For hydrogen sensing, a thin film (~ 5 nm) of Pd was applied over the initial gold layer using a DC source. All thicknesses were measured in-situ by a quartz crystal microbalance.

### **3.3.2 Humidity Sensor Measurement System**

The experimental system designed to measure dew point and humidity is pictured in figure 2. The set-up consisted of a dew point generator with a referenced chilled-mirror hygrometer to produce accurate levels of moisture. The 60° SPR probe head was contained inside a temperature controlled incubator unit along with in-line temperature and pressure monitoring. Static experiments were also conducted in the initial characterization of the SPR probe, where the probe was dipped into solutions of interest and then rinsed in deionized water between samples.

### **3.3.3 Hydrogen Sensor Measurement System**

A schematic of the experimental SPR hydrogen measurement system is shown in figure 3. The SPR probe is constructed from 0.5 inch stainless tubing and may be Swage-Loc fitted into a process stream. Therefore, a flow cell was constructed from a 0.5 inch stainless tee, which would accommodate the SPR sensor in a flowing gas stream contained in a 0.125 inch diameter flow channel. The flow cell was constructed such that the 45° SPR sensing surface was placed in the center of the stream. The SPR probe was held in place with a Teflon ferrule and Swage-Loc bushing. Gas mixing and flow was controlled by the use of digitally controlled mass flow controllers (Aera Corporation).

## **3.4 Optical System**

The optical system consisted of the SPR probe (which contained ultra-violet (UV) grade 200 micron core diameter fibers for launch and collection of the light), light source, optical spectrometer and instrument controller. The SPR probe input fiber was coupled to a tungsten-halogen light source (Ocean Optics LS-1) while the collection fiber was inserted into a Ziess MCS 501 UV-Vis spectrometer. The spectrometer optical bench was obtained commercially and mated to internally developed data acquisition and analysis hardware/software. The spectrometer has 0.8 nm pixel resolution with approximately 4 nm optical resolution with a wavelength range from 190 to 1100 nm. The typical

experiment was performed using a 15-scan signal average in absorbance mode such that the SPR reflectivity minimum would display as a peak in the absorption spectrum when the system was referenced to air. The peak position was obtained dynamically after a 5 point Gaussian convolution smoothing filter using a least squares peak picking algorithm internal to the program. Data were logged onto a Micron GoBook II laptop computer with the Windows 98 operating system. The control software enabled various modes of data acquisition and full spectra along with a log file containing a time stamp and peak position were saved onto the computer hard drive for later retrieval and analysis. Data processing and analysis was performed using Matlab™ (The Mathworks, Inc.) and Microcal Origin 6.1 software (Originlab Corporation).

## 4.0 RESULTS AND DISCUSSION

### 4.1 SPR Probe Characterization

An SPR experiment requires that the optical reflectivity be measured at the sensor/liquid interface, and this in turn requires some reference beam, which approximates the lamp intensity after it has traversed the optical system. This can be achieved with the SPR probe by exposing the sensor to air, which does not generate a plasmon resonance, and recording the reference spectrum prior to performing liquid experiments. The probe design is such that rotation of the hemisphere, which is held in place by a screw cap sealed with Viton o-rings, causes slight shifts in the resonance due to imperfections in the machining of the probe as well as non-uniformity in the gold layer. It is important; therefore, that the screw cap be tightened sufficiently and that the referencing procedure be performed in the cell, after the Swage-Loc fittings have been tightened. This procedure provides a reference spectrum, which is representative of the optical system and therefore increases the quality of the SPR spectrum obtained when sample is passed over the sensor.

Figure 4 displays a comparison between the SPR spectrum obtained in deionized water at 30°C with a theoretical spectrum calculated from the material optical constants, gold thickness, and refractive index of water. The theoretical spectrum was calculated from known optical constants for the materials making up the three layer optical structure (fused-silica, gold, and water) using a Matlab™ script based on the calculation of the Fresnel reflection coefficients for the structure using a matrix formalism<sup>9</sup>. The gold thickness was varied during modeling in order to determine by comparison the actual gold thickness on the hemisphere. The SPR sensor gold thickness determined from the position of the resonance is approximately 440 Å while the target deposition thickness was 550 Å. The 110 Å difference between the measured and target thicknesses can be attributed to errors in the thickness monitor due to proximity of the sample and thickness monitor inside the vacuum chamber during deposition.

The difference in magnitude of the resonance between the experimental and theoretical plots is due to the nature of the optical system and the referencing method. The calculation to obtain the theoretical curve is analogous to a reflectivity calculation, or simply  $I/I_0$ , where the source intensity profile is taken as  $I_0$ . Therefore, the reflectivity is a

convolution of the SPR feature, shown as a sharp minimum at around 580 nm, and the reflectivity of gold metal, which is lower in the blue end of the spectrum due the absorption of gold, giving it its yellow hue. The experimental curve was generated with a real reference of the optical system through the SPR probe and the reference spectrum, therefore, was attenuated by the gold at lower wavelengths. This is why the SPR spectrum from the SPR probe referenced to air is symmetrical and the reflectivity approaches unity away from the resonance. In addition, the establishment of a resonance requires that the polarization state of the input beam contain transverse magnetic components (TM or p-polarized). If the polarization state is pure, and the metal film is the correct thickness, the reflectivity at the resonance approaches zero. The theoretical calculations used in the generation of the theoretical curve assumes pure p-polarized light. Conversely, the experimental SPR spectrum was obtained using a white light source with no polarizing optics. The orthogonal polarization states, transverse electric (TE, or s-polarized) and transverse magnetic, p-polarized, are present in roughly equal proportion due to the isotropic and random nature of the tungsten emission. In addition, any stable polarization state emitted from the lamp would be lost in the fibers due to randomization in the fiber core. The p-polarized components of the incident light would excite the plasmon oscillation while the s-polarized light returns unmodified to the detector. Therefore, the reflectivity minimum limit for 50:50 mixed polarization is 0.5. The minimum reflectivity in the experimental spectrum is approximately 0.65, indicating that some polarization of the beam is occurring, most likely due to the small air gap between the fiber end face and the hemisphere flat.

A key measure in determining the quality of the SPR spectrum is the full width at half maximum (or minimum) (FWHM) of the resonance. Broadening of the resonance is generally caused by poor collimation of the incident beam in white light experiments. The curvature of the hemisphere compensates for the divergence of the optical fibers and fixes the incident angle at  $60^\circ$ , with very little off-axis light striking the interface. The fact that there is essentially no broadening in the resonance with respect to the theoretical FWHM indicates the probe is generating high resolution, low noise SPR spectra. This is important in that the limit of detection for surface adsorbed species is a function of how well one determines the position of the resonance. The ability to distinguish small shifts in the resonance degrades as the resonance broadens.

Stable SPR positions were used in a second order polynomial least squares fit of the refractive index at  $30^\circ\text{C}$  to the SPR wavelength values for each solution. Figure 5 displays the relationship between the SPR wavelengths and the refractive indices of the various calibration solutions. The curve is consistent with the non-linear response characteristic of SPR sensors<sup>10</sup>. As the resonance wavelength increases, the sensitivity increases as well. The probe sensitivity to refractive index may be calculated from the regression coefficients around a specific wavelength which, for small shifts will be approximately linear. The sensitivity calculated near the refractive index of water is  $9.9 \times 10^{-4}$  refractive index units (RIU) per nm, or 1010 nm/RIU. This slope increases with SPR wavelength, and operation at longer wavelengths would provide increased sensitivity to changes in refractive index. However, this sensitivity is comparable to other SPR system reported in the literature<sup>10, 11</sup> and is suitable for surface absorption studies.

## 4.2 Evaluation of Sensor Coatings

### 4.2.1 *Silicon Dioxide Coatings*

Experiments were conducted using a 60° incident angle probe to examine the effects of water sorption into and on silicon dioxide thin films. After coating the apex of fused-silica hemispherical lenses with gold, thin films of silicon dioxide were sputter deposited under vacuum conditions. SiO<sub>2</sub> has been shown to effectively adsorb moisture onto its surface and into its porous structure. This process of water adsorption changes the optical constants and thickness of the SiO<sub>2</sub> layer thus causing changes in the SPR minimum.

After initial characterization, the sensor was subjected to various controlled humidity environments in order to test the sensitivity of the SPR sensor to adsorbed moisture. The sensor was placed in a large chamber with a recycling pump, drying tube and ultrasonic generator capable of generating humidity in the range of 10% to 100% relative humidity (RH). The chamber humidity was incrementally stepped via computer control to test the response of the SPR sensor (Figure 6A-D). Shown in figure 6A-B is the response of the sensor to a short-term ramp (60 min.) and the corresponding SPR wavelength change over the ramp period. Figures 6C-D demonstrate the long-term (18 hrs.) response of the same probe. The sensor showed a response sensitivity of 0.025% RH which compares well to commercial humidity sensors with sensitivities commonly at 1.0% RH. The data also indicates that the sensor system operates reproducibly over a wide range of humidity levels with the relative error being 0.92% and 1.05% for the short and long-term ramps respectively. Stabilization of the probe signal (i.e. reducing hysteresis and long-term drift) can be improved by minimizing stress in the silica film. This can be accomplished by varying the deposition parameters, which could possibly produce more porous silica films which would be less susceptible to compressive stresses induced by water adsorption. Also, simply heating the film could reduce lattice stresses on silicon oxide bonds that are more active than relaxed bonds.

To facilitate testing the SPR probe in low humidity settings, a second experimental system was assembled which included a NIST-traceable chilled-mirror hygrometer. The SPR moisture probe was tested over a 49-day period and the temperature corrected response is shown in figure 7. One can observe that the SPR predicted dewpoints trended very linearly with the referenced dewpoint measurements. Additionally, the experimental data demonstrated that the probe was sensitive to 0.75 parts-per-million dewpoint or 0.005% RH.

### 4.2.2 *Palladium Hydride Coatings*

In order to develop a hydrogen sensor based upon palladium thin films, an understanding of the selective interaction between hydrogen and palladium is necessary. This report focuses on the adsorption and desorption of hydrogen in thin palladium films (<100nm) at room temperature and pressure. For a thorough discussion of the palladium/hydrogen system consult Lewis<sup>12</sup>. Butler et al have demonstrated that adsorption of hydrogen in

thin palladium films at room temperature and pressure leads to reversible hydrides of the form  $\text{PdH}_x$  where  $x$  is the atomic ratio  $\text{H/Pd}$ <sup>13</sup>. The 'pressure-composition' isotherm of the palladium/hydrogen adsorption is shown in Figure 8 and represents the palladium crystallographic phase transition that occurs upon adsorption of hydrogen. For each isotherm occurring below 300°C one can observe two-phase transitions at which the  $\text{H/Pd}$  ratio increases with pressure, separated by an isopressure region. The two phases are considered the  $\alpha$  and  $\beta$  phases existing at pressures respectively lower and higher than the isopressure region. The isopressure region is the phase transition  $\alpha \leftrightarrow \beta$  where both phases coexist without mixing. Without hydrogen and at low atomic  $\text{H/Pd}$  ratios, palladium is in the  $\alpha$  phase and can be considered a very mobile dissolved form of  $\text{H}_2$ , while at larger  $\text{H/Pd}$  ratios palladium changes to the hydride  $\beta$  phase. Though the  $\beta$  phase  $\text{H/Pd}$  interaction has been shown to be very useful for hydrogen storage applications, research has shown that the absorption/desorption of palladium hydrides can cause considerable strain on the Pd lattice resulting in adhesion difficulties<sup>14</sup>, lattice dislocation<sup>12</sup>, and surface blistering<sup>15</sup>; all of which can be very detrimental to sensor performance.

Figure 9 represents the typical detection signal for successive cycles from a pure nitrogen atmosphere to a mixture of 4% hydrogen in nitrogen. The side of a 45° incident angle probe was metallized with a stack layer of Au and Pd by DC sputter deposition. The absorption of hydrogen by the Pd film will causes a change in the optical properties (i.e. dielectric constant) of the film, resulting in a change in the propagation properties of the surface plasmon (i.e. change in the reflectance)<sup>16</sup>. The thickness of the Pd has an influence on the light coupling into the SP wave, in addition to effecting the time necessary for the diffusion of hydrogen into the palladium layer (i.e. response time). Therefore a thickness of 5.0 nm was chosen to achieve a compromise between the level of response and the response time as observed from optical modeling and diffusion values for  $\text{H}_2$  into Pd thin films. The response time was shown to vary with  $\text{H}_2$  concentration being 600-s, 540-s, 420-s respectively, for the 2%, 3% and 4% concentration levels. The response and the response time are dependent upon the crystallographic phase transition of the  $\text{H/Pd}$  interaction<sup>17</sup>. This dependence on the crystallographic phase transition caused a non-linear response as observed in figure 9. This response is typical of the  $\text{H}_2$  sensors utilizing Pd thin films and can be addressed through the use of non-linear algorithms. At concentrations between 1-3%  $\text{H}_2$ , the palladium was in the  $\alpha \leftrightarrow \beta$  phase transition, where large changes in response and long response times were observed. At concentrations greater than 3%  $\text{H}_2$ , the palladium was predominately in the  $\beta$  phase, where minimal response variation and a decrease in response time were observed. Attempts to reasonably change the response and recovery times by varying the temperature of the measurements from 25 – 50°C were inconclusive. This is predominately due to the slow diffusion of hydrogen through thick Pd film layers. The authors attribute this to errors in the measured film thickness due to the difficulties involved in the accurate calibration of the thickness monitoring system for sputter deposition. Nevertheless, the sensor demonstrated sensitivity down to 1% (data not shown) and by extrapolating the data to zero, a detection limit of 0.102% ( $S/N = 3$ )  $\text{H}_2$  was calculated.

## **5.0 CONCLUSIONS AND FUTURE WORK**

We have demonstrated two successful applications of a monolithic SPR probe. The simple optical design of the device increased robustness and fabrication precision and allowed for sensitive SPR measurements to be made without complex polarizing and collimating optics. For moisture sensing, the probe demonstrated a large dynamic range from less than one part per million (0.005% RH) to greater than 20,000 parts per million (approx. 100% RH) dewpoint by weight. This device was also capable of optically detecting hydrogen concentrations from at least 0.1% to the lower explosive limit (4%) with a calculated limit of detection for H<sub>2</sub> of 0.102% (S/N=3 criteria). While further improvements are needed in the sensing films before process use is suggested, this sensor has shown to provide sensitive, selective and intrinsically safe moisture and hydrogen measurements for hazardous environments.

It is the opinion of the authors that continued research and development in the area of polymeric thin films should be pursued. Novel thin film technologies such as molecularly imprinted polymers would couple well with SPR spectroscopy to provide highly selective probes for moisture, ammonia and many other process gas phase contaminants. This would not only lead to inexpensive, robust process measurement probes, but would expand the core competency of the Savannah River Site.

## **6.0 ACKNOWLEDGEMENTS**

The authors would like to thank D. Pak of ADS for design and fabrication of aluminum alignment and coating masks.

## 7.0 REFERENCES

- (1) Spencer, W. A., Tovo, L.L.; Westinghouse Savannah River Company: Aiken, **2003**, WSRC-TR-2002-00554.
- (2) Nelson, B. P., Frutos, A.G., Brockman, J.M., Corn, R.M. *Analytical Chemistry* **1999**, *71*, 3928.
- (3) Nelson, B. P., Frutos, A.G., Brockman, J.M., Corn, R.M. *Analytical Chemistry* **1999**, *71*, 3935.
- (4) Jorgenson, R. C., Yee, S.S. *Sensors and Actuators* **1993**, *B12*, 213.
- (5) Jorgenson, R. C., Yung, C., Yee, S.S., Burgess, L.W. *Sensors and Actuators* **1993**, *B13-14*, 721.
- (6) Slavik, R., Homola, J., Ctyroky, J. *Sensors and Actuators* **1999**, *B54*, 74.
- (7) Stemmler, I., Brecht, A., Gauglitz, G. *Sensors and Actuators* **1999**, *B54*, 98.
- (8) Weast, R. C., Ed. *CRC Handbook of Chemistry and Physics*, 1989.
- (9) Karlsen, S., University of Washington, Seattle, 1994.
- (10) Homola, J., Yee, S.S., Gauglitz, G. *Sensors and Actuators* **1999**, *B54*, 3.
- (11) Johnston, K. S., Booksh, K.S., Chinowsky, T.M., Yee, S.S. *Sensors and Actuators* **1999**, *B54*, 80.
- (12) Lewis, F. A. *The Palladium Hydrogen System*; Academic Press Inc.: London, 1967.
- (13) Butler, M. A. *Applied Physics Letters* **1984**, *45*, 1007.
- (14) Shivaraman, M., Svensson, C. *Journal of the Electrochemical Society* **1976**, *125*, 1258.
- (15) Armgarth, M., Nylander, C. *IEEE Electronic Device Letters* **1982**, *EDL-3*, 384.
- (16) Chadwick, B., Gal, M. *Applied Surface Science* **1993**, *68*, 135.
- (17) Bevenot, X., Trouillet, A., Veillas, C., Gagnaire, H., Clement, M. *Measurement Science Techonolgy* **2002**, *13*, 118.



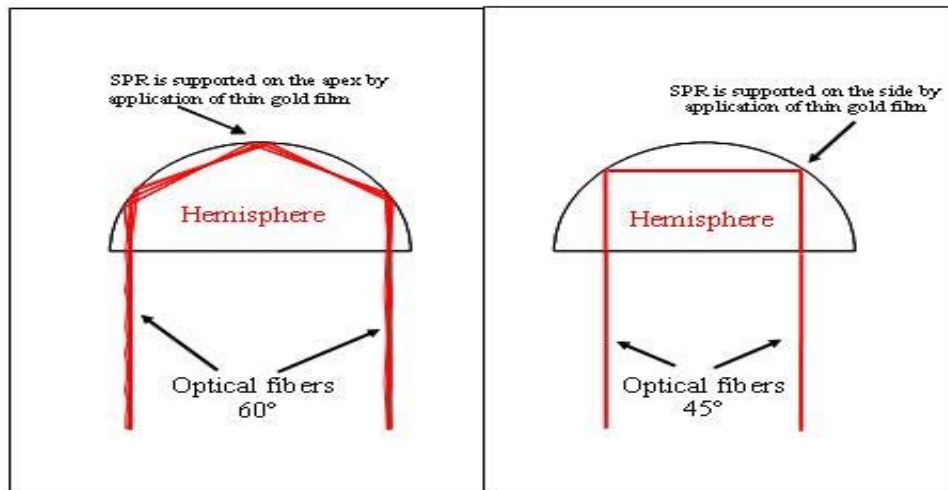


**Figure1. Optical ray-trace of the 60° and 45° SPR probes. The probes were fabricated using a commercially available attenuated total reflection spectroscopy probe. Optical fibers deliver the incident light to the flat face of the hemisphere and then collect the reflected light. The incident angle is held constant by the curvature of the optic for both the two and three bounce probes. This structure represents the first monolithic, high resolution fiber optic SPR probes.**

**Table 1. Standard salt solutions used in Characterization of the SPR sensor to refractive index perturbations.**

NaCl weight	Total solution weight	wt. % NaCl	Refractive index, 20°C, at sodium d-line	Refractive index at 30°C, sodium d-line
0.0000	100.000	0.000%	1.33291	1.33174
0.5003	100.887	0.496%	1.33379	1.33262
0.9996	100.044	0.999%	1.33468	1.33351
2.0001	100.154	1.997%	1.33646	1.33529
3.0008	100.067	2.999%	1.33823	1.33706
3.9930	100.179	3.986%	1.33998	1.33881
5.0007	100.098	4.996%	1.34178	1.34061
6.0044	100.146	5.996%	1.34355	1.34238
7.0024	100.011	7.002%	1.34534	1.34417
8.0030	100.038	8.000%	1.34711	1.34594
9.0031	100.142	8.990%	1.34887	1.34770
10.0011	100.133	9.988%	1.35064	1.34947
12.0011	103.126	11.637%	1.35356	1.35239
14.0089	99.993	14.010%	1.35777	1.35660
16.0029	100.048	15.995%	1.36130	1.36013
18.0041	100.008	18.003%	1.36486	1.36369
20.0078	100.085	19.991%	1.36839	1.36722

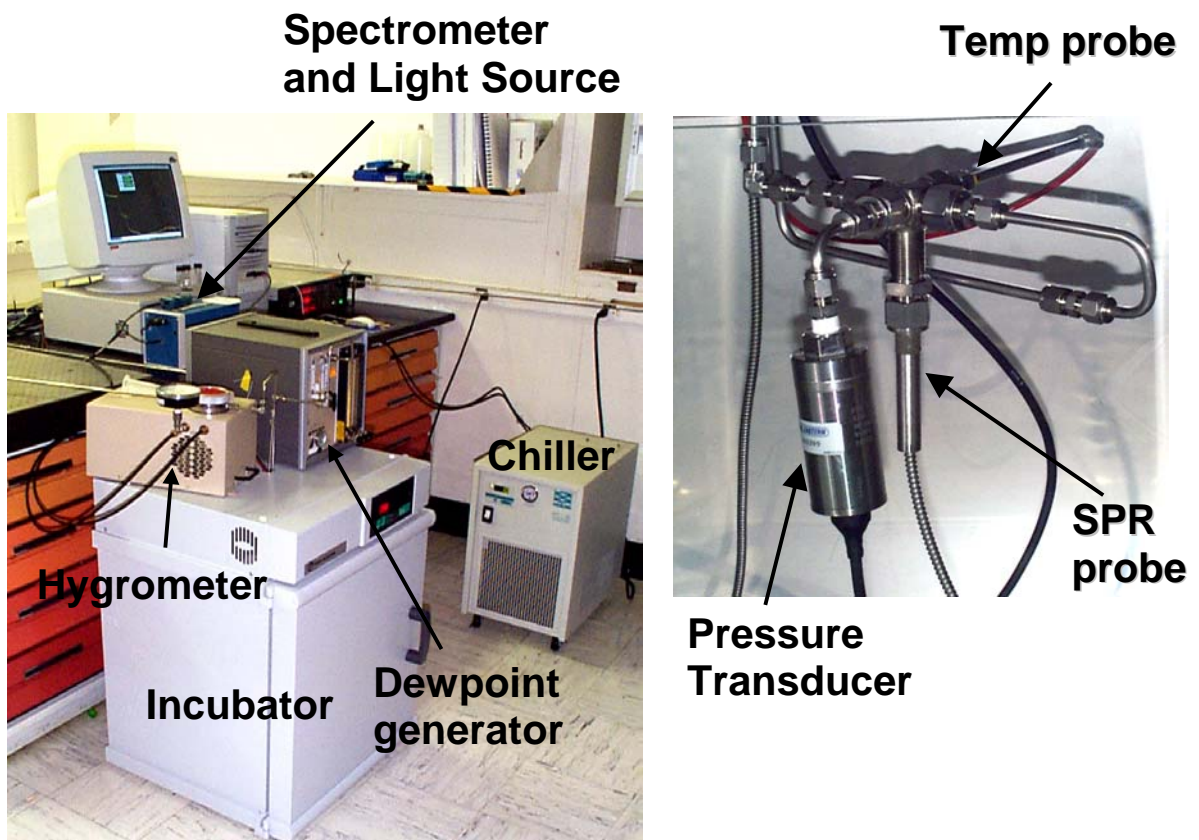
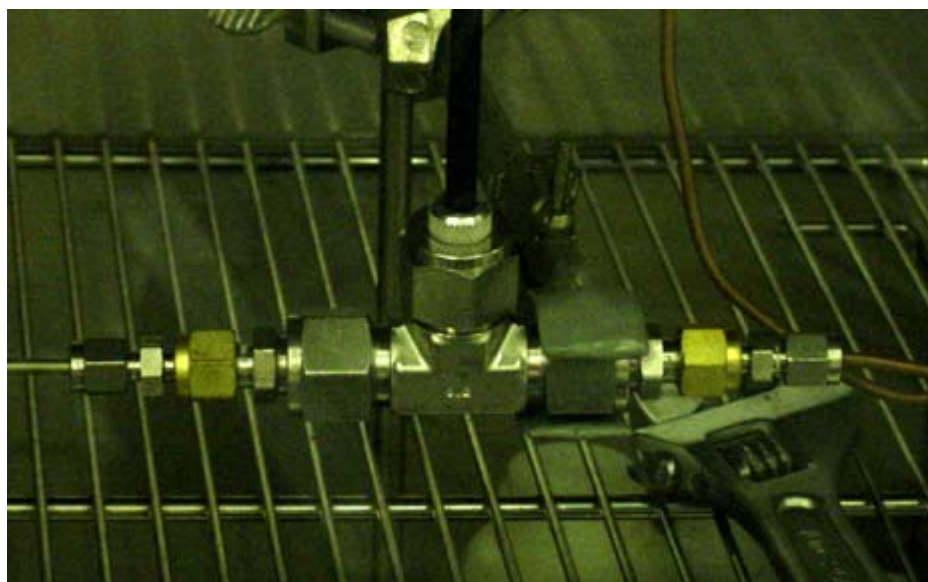
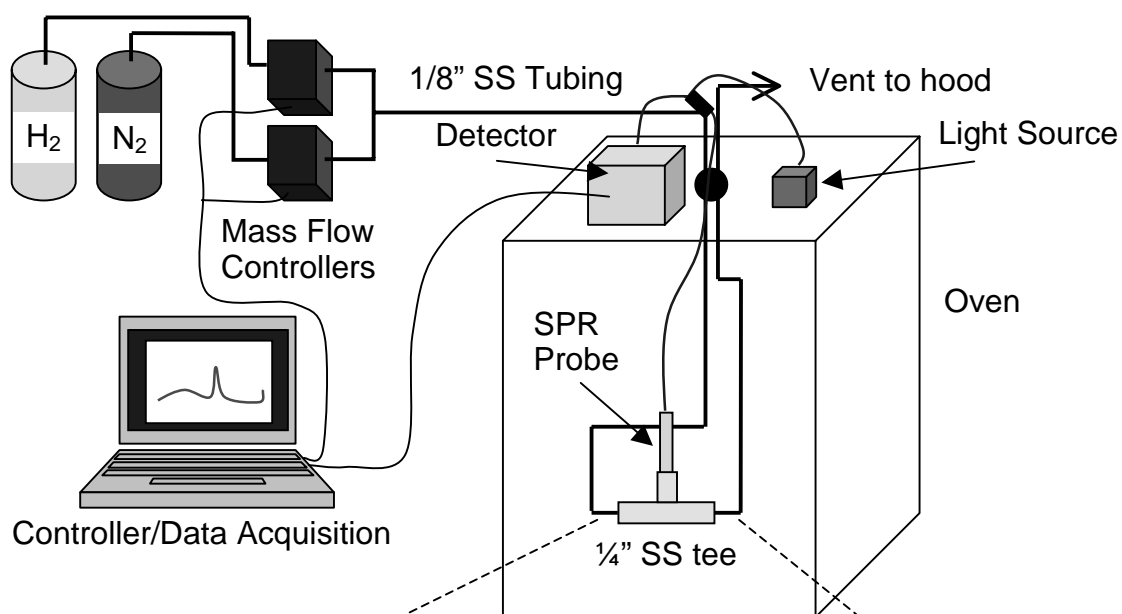
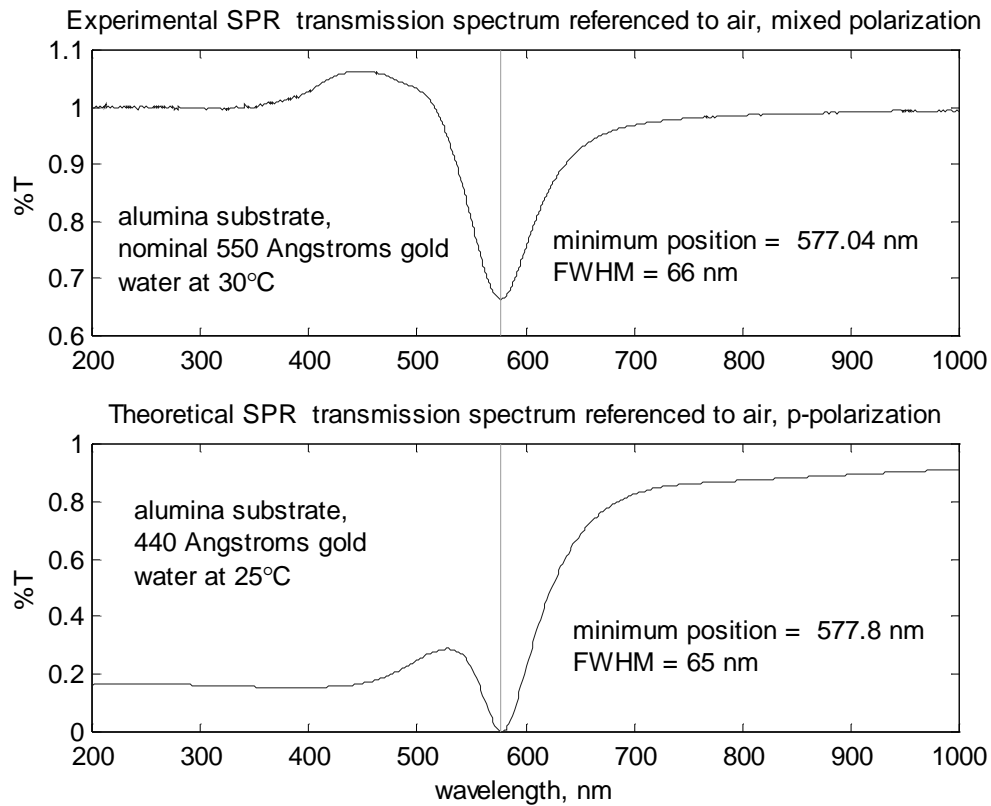


Figure 2. Experimental set-up for the measurement of dew point and humidity.



**Figure 3. Experimental apparatus for the detection of hydrogen.**



**Figure 4. Comparison between experimental (above) and theoretical (below) SPR spectra; shows that the SRTC fiber optic SPR probe generates high quality, high resolution spectra.**

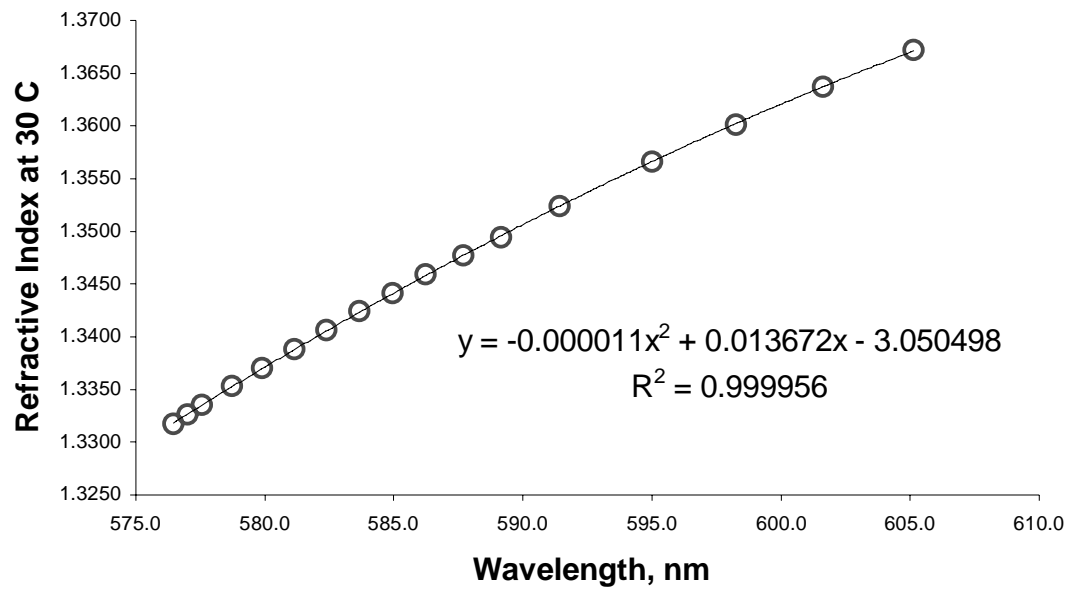


**Figure 5. SPR sensor refractive index calibration; results show the non-linear relationship between the SPR wavelength and refractive index of the sample.**

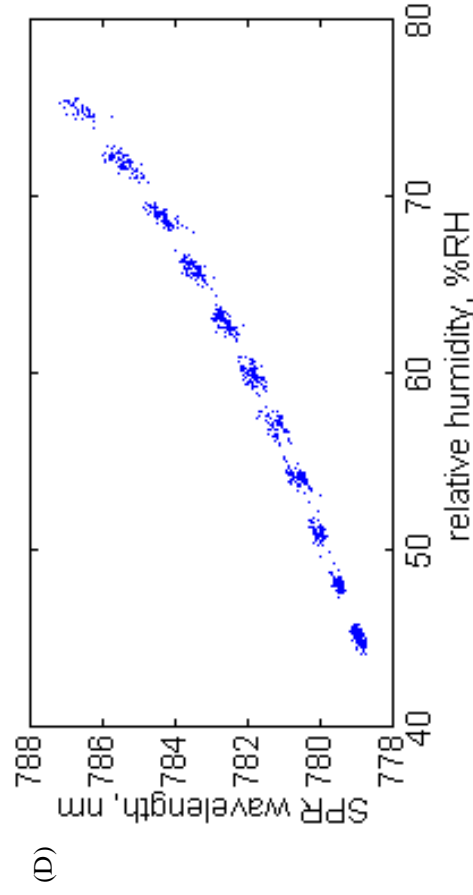
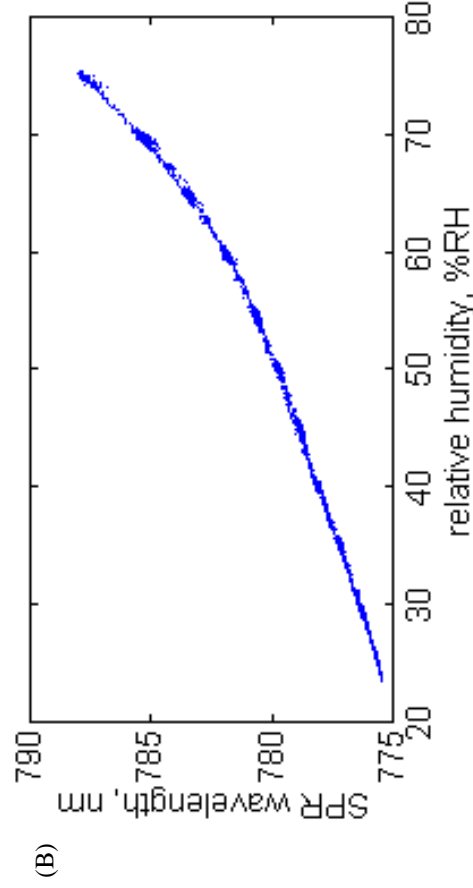
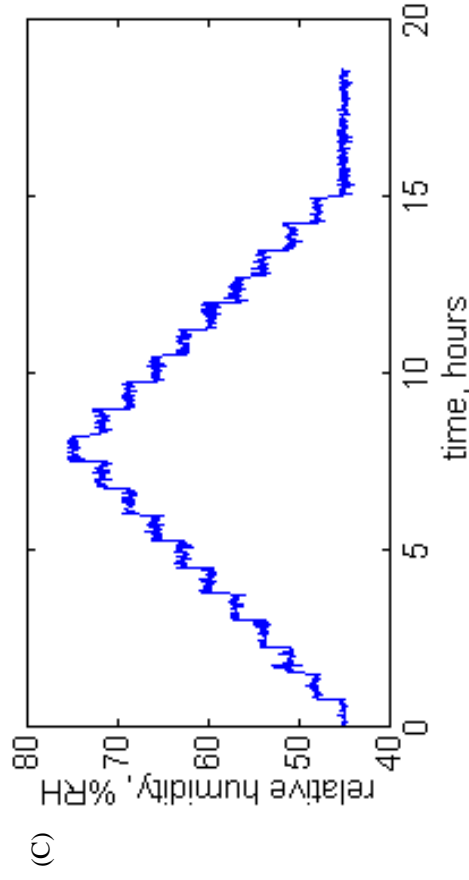
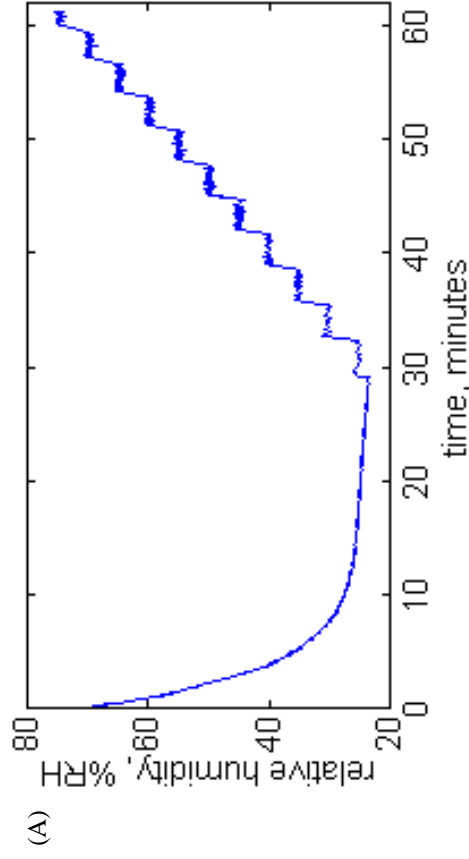


**Figure 6. Short-term (A-B) and long-term (C-D) comparisons of the resonance wavelength obtained from the gold/silica sensor with the baseline humidity values from a capacitive RH sensor.**

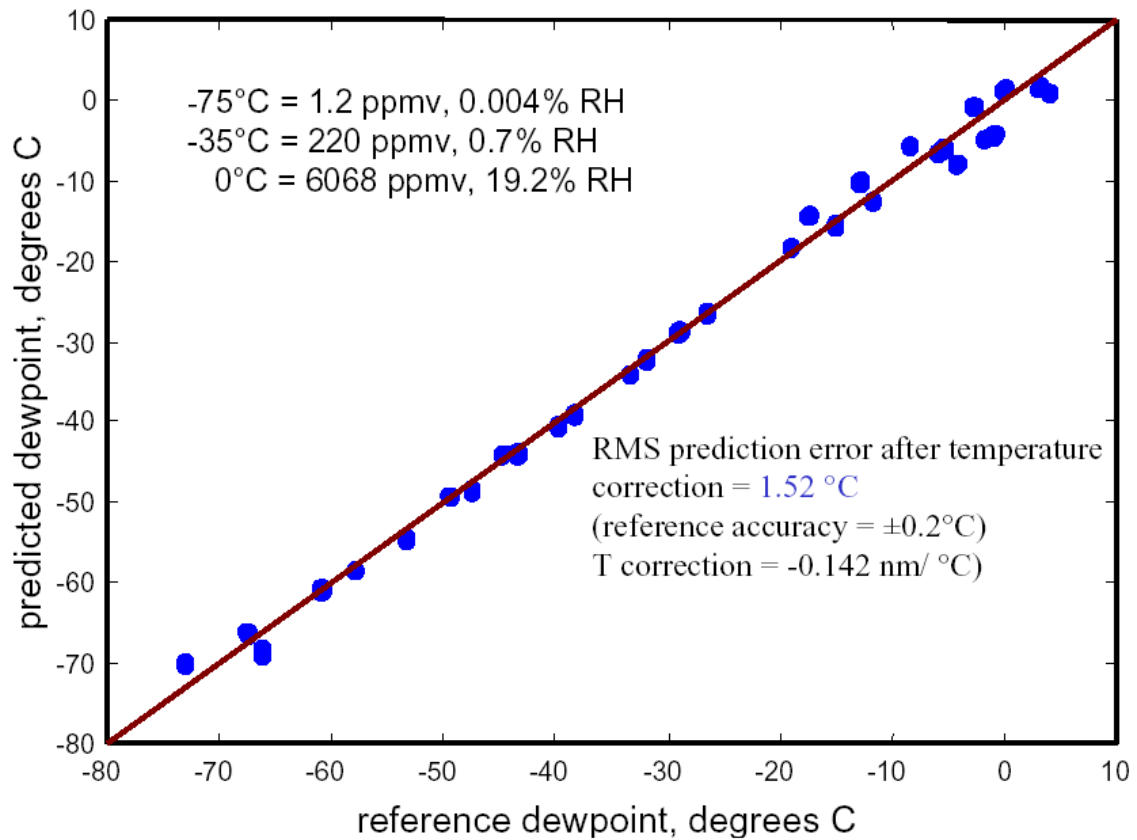


**Figure 7. Prediction results for 49 day trial, temperature corrected SPR moisture sensor.**



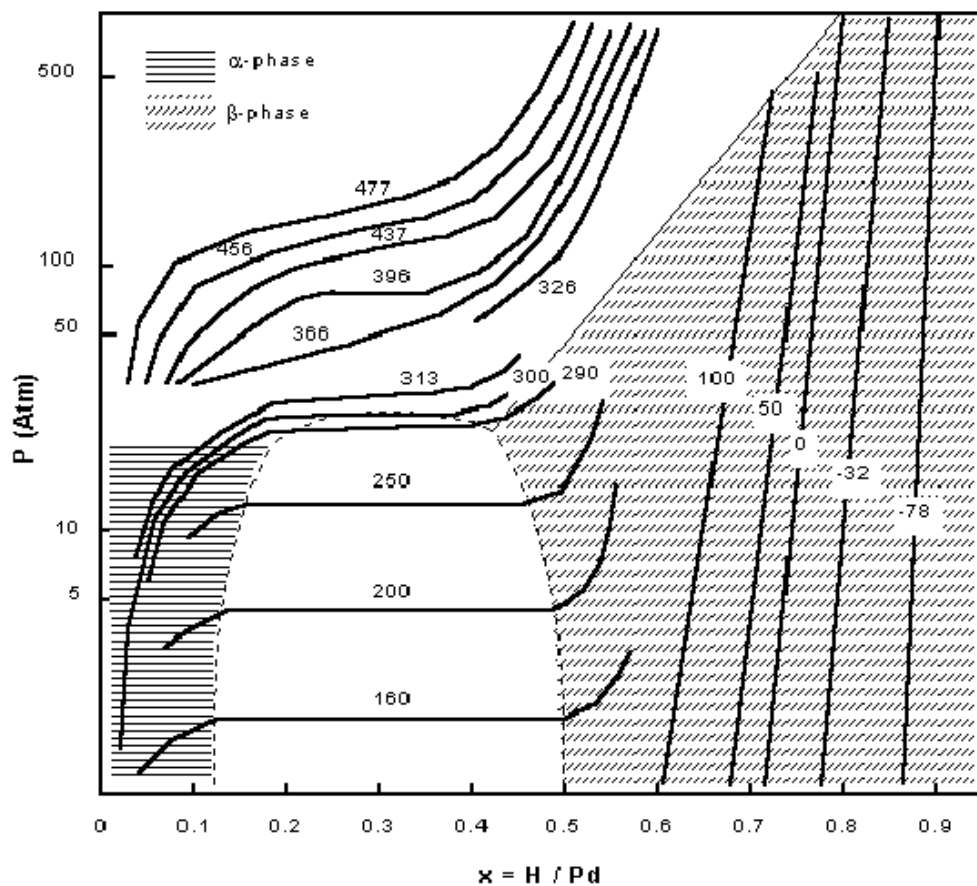
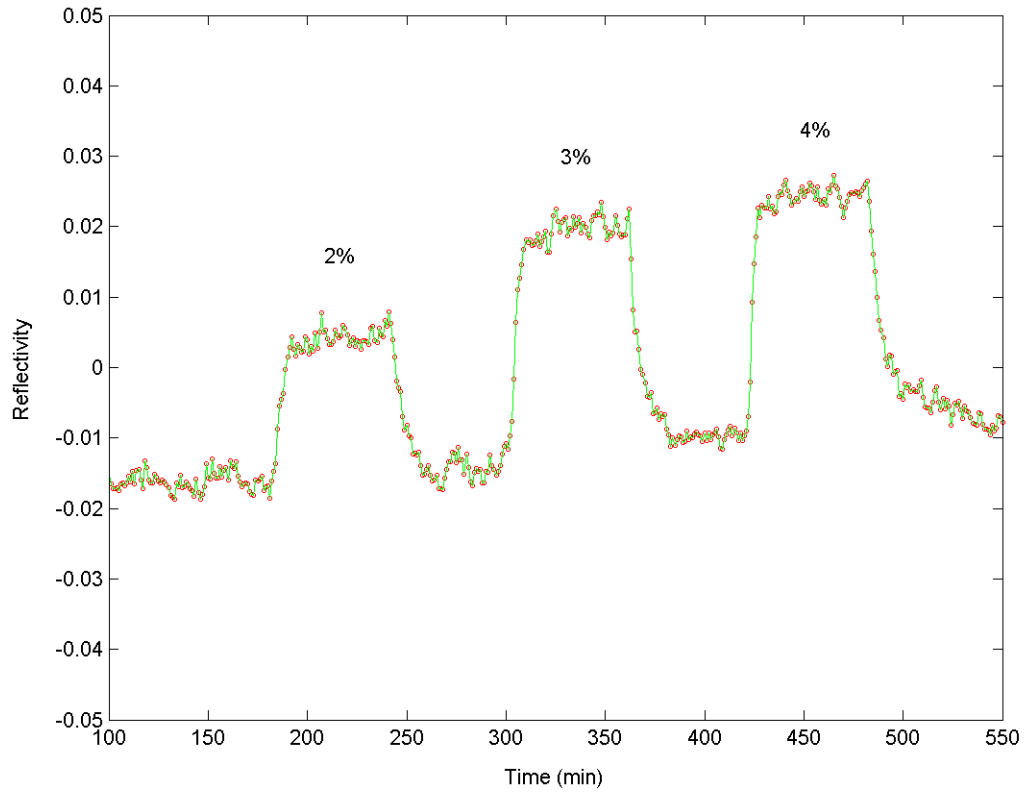


Figure 8. “Pressure-composition” isotherms for palladium versus the absorption of molecular hydrogen for various temperatures in degrees Celsius (from Lewis et. al.).



**Figure 9. Typical response for successive cycles from pure nitrogen to a 4% hydrogen concentration.**